Metastable decoherence-free subspace and pointer states in mesoscopic quantum systems

F. Lastra,[1] C. E. López,[2] and J. C. Retamal[2,3]

[1]*Departamento de Física, Facultad de Ciencias Básicas, Universidad de Antofagasta, Casilla 170, Antofagasta, Chile*

[2]*Departamento de Física, Universidad de Santiago de Chile, USACH, Casilla 307 Correo 2 Santiago, Chile*

[3]*Center for the Development of Nanoscience and Nanotechnology, 9170124, Estación Central, Santiago, Chile*

(Received 4 February 2018; published 24 April 2018)

Two initially correlated coherent states, each interacting with its own independent dissipative environment, exhibit a sudden transition from classical to quantum decoherence. This change in the dynamics is a turning point in the decoherence in the sense that depending on the average number of photons of each harmonic oscillator, decoherence can even be suppressed. Indeed, the quantum state is time independent for a time span in the mesoscopic regime, revealing a decoherence-free subspace. Furthermore, the absence of decoherence is manifested in the apparition of a metastable pointer-state basis.

DOI: 10.1103/PhysRevA.97.042123

I. INTRODUCTION

The study of quantum correlations in multipartite quantum systems is a central problem in quantum mechanics. The study of all correlations existing between two quantum systems, not only entanglement, has captured the attention of many researchers in recent years. Quantum and classical correlations embodied in a bipartite quantum system are contained in the quantum mutual information [1,2]. From this fundamental concept, the search of all quantum correlations that can be found in a bipartite system has motivated the introduction of quantum discord [2–7]. One main result driving research in this field is that quantum computation is possible even in the absence of quantum entanglement [8].

A central issue is the understanding of how a bipartite system behaves under the interaction with an environment. Concerning this effect, it is widely known that entanglement could vanish suddenly, depending on the initial state [9–13]. Given that, it is important to know how quantum correlations, other than entanglement, are affected by the presence of environment [14–18]. Both classical and quantum correlations are affected such that in most cases, they decay asymptotically, independent of the initial state, and this feature distinguishes them from quantum entanglement. As the total mutual information decays as a function of time, it could be interesting to see how this decay can be associated to classical or quantum correlations. An unexpected behavior has been revealed for a certain class of quantum states evolving under dephasing: Their classical correlations decay, while the quantum correlations remain constant. This is followed by an exchange in the roles, that is, decaying of quantum correlations and freezing of classical correlations [19,20]. These findings have been experimentally observed for non-Markovian and Markovian reservoirs [21,22]. Freezing of classical correlations has been shown in nondissipative decoherence dynamics [23,24]. Moreover, such behavior reveals the apparition of a pointer basis [2,3,22,24–26].

On the other hand, coherent states and environment effects on its quantum coherence have been one of the most important problems since the beginning of quantum mechanics. A distinctive feature concerning its dynamical behavior is the appearance of a decoherence timescale depending on the distance between coherent states, which is much shorter than the decay of any other observables [27,28]. Moreover, in recent years, these states have proven to be useful in practical applications such as quantum metrology [29–31]. In this paper, we address the evolution of quantum and classical correlations of an initially incoherent superposition of entangled coherent states. We find different timescales that give rise to a wide variety of behaviors, in particular, we observe sudden transitions in the decoherence dynamics. Moreover, measuring on one of the parties (to calculate classical correlations) projects the other into a basis which is not affected by decoherence. This reveals the apparition of metastable pointer states and a decoherence-free subspace whose time span depends on the amplitude of the initial coherent states.

II. PHYSICAL MODEL

To find such features, let us first consider the problem of a quantized harmonic oscillator coupled to a dissipative reservoir. In the interaction picture, the Hamiltonian of this system is given by

$$\hat{H}_I = \hbar \sum_k g_k (\hat{a}^\dagger \hat{b}_k e^{i(\nu - \nu_k)t} + \hat{a} \hat{b}_k^\dagger e^{-i(\nu - \nu_k)t}). \tag{1}$$

If the harmonic oscillator is prepared initially in a coherent state $|\alpha\rangle$ while all reservoir modes are in the vacuum state $\prod_k |0_k\rangle$, the evolution of the system will take the form

$$e^{-i\hat{H}_I t/\hbar} |\alpha\rangle \prod_k |0_k\rangle = |\alpha e^{-\gamma t/2}\rangle \prod_k |\alpha_k\rangle, \tag{2}$$

with γ the decay rate of the harmonic oscillator. The state $|\alpha_k\rangle$ denotes a coherent state for the kth mode of the reservoir with amplitude $\alpha_k = f_k \alpha$. In the Markov approximation, the factors f_k satisfy the relation $\sum_k f_k^2 = 1 - e^{-\gamma t}$ [32].

Consider now two noninteracting field modes (a and b), affected by two independent dissipative reservoirs. Let us assume both harmonic oscillators are prepared initially in an

incoherent superposition such as

$$\hat{\rho}_{ab}(0) = p|\psi_0^+\rangle\langle\psi_0^+| + (1-p)|\phi_0^+\rangle\langle\phi_0^+|, \tag{3}$$

where

$$|\psi_0^\pm\rangle = \frac{1}{\Lambda_\pm}(|\alpha\rangle_a|\alpha\rangle_b \pm |-\alpha\rangle_a|-\alpha\rangle_b), \tag{4}$$

$$|\phi_0^\pm\rangle = \frac{1}{\Lambda_\pm}(|\alpha\rangle_a|-\alpha\rangle_b \pm |-\alpha\rangle_a|\alpha\rangle_b), \tag{5}$$

and the normalization factor is given by $\Lambda_\pm^2 = 2(1 \pm e^{-4\bar{n}})$.

III. DYNAMICS OF QUANTUM AND CLASSICAL CORRELATIONS

In what follows, we deal with the calculation of quantum and classical correlations of the system described as a function of time. In general, this is a difficult task since no closed formula exists for arbitrary states. However, for particular states such as X states [33,34], analytical calculations can be carried out. After some calculations, it is not difficult to realize that the temporal evolution for the state (3) can be written as X states in the effective two-qubit basis: $\{|\eta_+\rangle_a|\eta_+\rangle_b, |\eta_+\rangle_a|\eta_-\rangle_b, |\eta_-\rangle_a|\eta_+\rangle_b, |\eta_-\rangle_a|\eta_-\rangle_b\}$, where states $|\eta_+\rangle(|\eta_-\rangle)$ are commonly known as Schrödinger cat states [27,28],

$$|\eta_\pm\rangle = \frac{1}{\Gamma_\pm}(|\alpha_t\rangle \pm |-\alpha_t\rangle), \tag{6}$$

with $\alpha_t^2 = \bar{n}\exp(-\gamma t)$. In such basis, we obtain the following X state:

$$\rho_{ab}(t) = \begin{pmatrix} r_{11} & 0 & 0 & r_{14} \\ 0 & r_{22} & r_{23} & 0 \\ 0 & r_{32} & r_{33} & 0 \\ r_{41} & 0 & 0 & r_{44} \end{pmatrix}, \tag{7}$$

where the matrix elements are

$$\begin{aligned} r_{11} &= \frac{1}{16}\left[\frac{\Gamma_+(t)\Gamma_+(t)}{\Lambda_+}\bar{\Lambda}_+(t)\right]^2, \\ r_{22} &= \frac{1}{16}\left[\frac{\Gamma_+(t)\Gamma_-(t)}{\Lambda_+}\bar{\Lambda}_-(t)\right]^2 = r_{33}, \\ r_{44} &= \frac{1}{16}\left[\frac{\Gamma_-(t)\Gamma_-(t)}{\Lambda_+}\bar{\Lambda}_+(t)\right]^2, \\ r_{14} &= r_{41} = \frac{1}{16}(2p-1)\left[\frac{\Gamma_+(t)\Gamma_-(t)}{\Lambda_+}\bar{\Lambda}_+(t)\right]^2, \\ r_{23} &= r_{32} = \frac{1}{16}(2p-1)\left[\frac{\Gamma_+(t)\Gamma_-(t)}{\Lambda_+}\bar{\Lambda}_-(t)\right]^2, \end{aligned} \tag{8}$$

with $\Gamma_\pm^2 = 2[1 \pm \exp(-2\alpha_t^2)]$, $\bar{\Lambda}_\pm^2(t) = 2(1 \pm e^{-4\bar{\alpha}_t^2})$, and $\bar{\alpha}_t^2 = \bar{n}(1 - e^{-\gamma t})$.

A closer look at these analytical expressions can shed some light on the relevant timescales. As will be shown below, the dynamics exhibits different behaviors associated to these relevant times. The evolution of the matrix elements in Eq. (8) is mainly determined by the terms α_t^2 and $\bar{\alpha}_t^2$ in the exponentials. On one hand, as time goes by, we see that the value of α_t decreases, leading to a slower decay of terms involving $e^{-\alpha_t^2}$. On the other hand, the value $\bar{\alpha}_t^2$ increases, leading to a faster decay of terms involving $e^{-\bar{\alpha}_t^2}$. However, in the mesoscopic limit $\bar{n} \gg 1$, at short times the term α_t is large enough so that $e^{-\alpha_t^2} \simeq 0$ and then the dynamics is dominated by the term $e^{-\bar{\alpha}_t^2}$. This means that the time dependence in Eq. (8) is only in the terms $\bar{\Lambda}_\pm(t)$, while $\Gamma_\pm(t)$ are constant. On the other hand, when $\gamma t \to \infty$, we have the opposite case: the dynamics is now governed by $\Gamma_\pm(t)$, while $\bar{\Lambda}_\pm(t)$ are constant. For intermediate times, both α_t and $\bar{\alpha}_t$ are large enough so that $\bar{\Lambda}_\pm(t)$ and $\Gamma_\pm(t)$ are both constant, so that the matrix elements given by

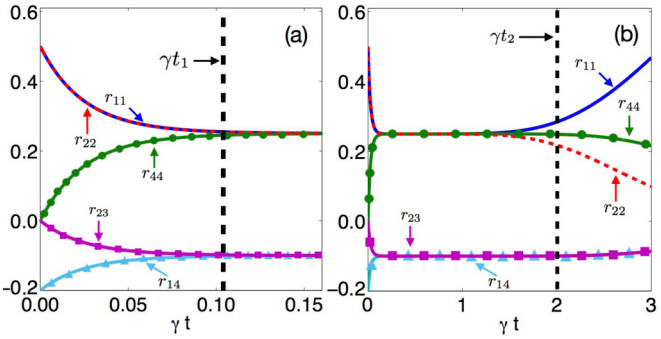

FIG. 1. Evolution of the density matrix elements r_{11}, r_{22}, r_{33} and r_{44} of Eq. (8) for $\bar{n} = 10$. The a-dimensional times γt_1 and γt_2 are in this case: $\gamma t_1 \simeq 0.1$ and $\gamma t_2 \simeq 2$ and are shown as vertical dashed lines.

$$r_{11} = r_{22} = r_{33} = r_{44} = \tfrac{1}{4}, \tag{9}$$

$$r_{14} = r_{41} = r_{23} = r_{32} = \tfrac{1}{4}(2p-1) \tag{10}$$

exhibit no evolution and depend only on the initial condition.

We can estimate the value of the times that define this dynamical regime. For large $\bar{n}$, the exponentials are relevant if $\alpha_t \lesssim 1$ or $\bar{\alpha}_t \lesssim 1$, respectively. This allows us to define the times t_1 from $\bar{\alpha}_{t_1} = 1$ and t_2 from $\alpha_{t_2} = 1$, such that

$$\begin{aligned} t_1 &= \frac{1}{\gamma}\ln\frac{\bar{n}}{\bar{n}-1}, \\ t_2 &= \frac{1}{\gamma}\ln\bar{n}. \end{aligned} \tag{11}$$

The evolution of the matrix elements in Eq. (8) is shown in Fig. 1, for $\bar{n} = 10$. Interestingly, between t_1 and t_2 we observe that the system seems to be unaffected by decoherence, that is, it settles on a *metastable decoherence-free subspace* evidenced by Eqs. (9) and (10). As we will address further in this manuscript, these results are crucial in the quantum and classical correlations dynamics.

We can now focus on the study of quantum and classical correlations. A bipartite quantum system $\hat{\rho}_{ab}$ such as the one described above can feature both quantum and classical correlations. Total correlations are characterized by the quantum mutual information $I(\hat{\rho}_{ab}) = S(\hat{\rho}_a) + S(\hat{\rho}_b) - S(\hat{\rho}_{ab})$, where $S(\hat{\rho}) = -\mathrm{Tr}[\hat{\rho}\log_2(\hat{\rho})]$ is the von Neumann entropy. Based on this expression, correlations can be separated according to their classical and quantum nature, respectively. In this way, the quantum discord has been introduced as $D(\hat{\rho}_{ab}) = I(\hat{\rho}_{ab}) - C(\hat{\rho}_{ab})$, which quantifies genuine quantum correlations; this

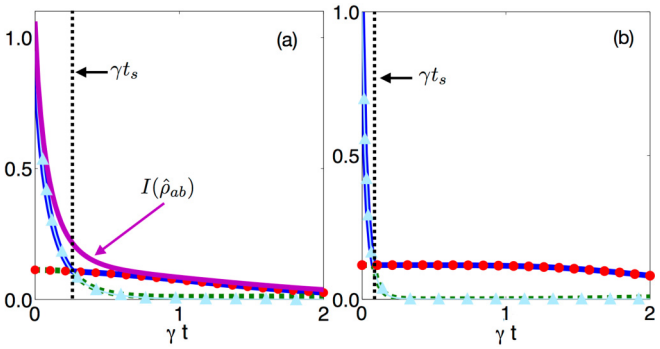

FIG. 2. Evolution of classical correlations (blue solid line), discord (green dashed line), and quantum mutual information (purple solid line) as a function of the dimensionless time γt for the initial state given by (3) with $p = 0.3$. (a) $\bar{n} = 1$. (b) $\bar{n} = 3$. $C(\hat{\rho_{ab}})|_{\sigma_x}$ (red dots) and $C(\hat{\rho_{ab}})|_{\sigma_z}$ (light blue triangles) are shown in both plots.

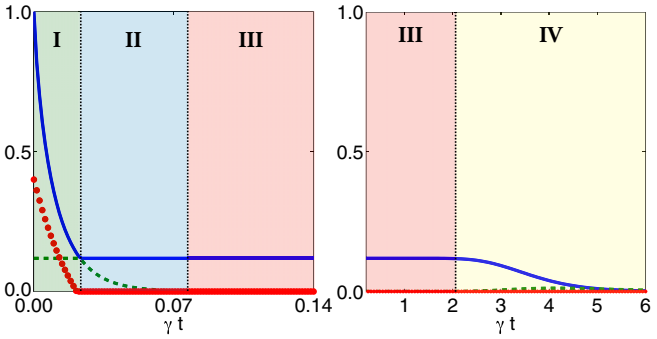

FIG. 3. Evolution of classical correlations (blue solid line), discord (green dashed line), and concurrence (red dots) as a function of the dimensionless time γt. The initial state is given by (3) with $p = 0.3$ and $\bar{n} = 10$. Left plot is for short times $\gamma t < 1$ and the right plot is for larger times.

includes correlations that can be distinct from entanglement. Here, $C(\hat{\rho}_{ab})$ are the classical correlations defined by [2–7]

$$C(\hat{\rho}_{ab}) = \max_{\{\hat{\Pi}_k\}}[S(\hat{\rho}_a) - S(\hat{\rho}_{ab}|\{\hat{\Pi}_k\})], \tag{12}$$

where the optimization is carried out with respect to all possible complete sets of projector operators $\{\hat{\Pi}_k\}$ for the subsystem b, and $S(\hat{\rho}_{ab}|\{\hat{\Pi}_k\}) = \sum_k p_k S(\hat{\rho}_k)$, $p_k = \mathrm{Tr}(\hat{\rho}_{ab}\hat{\Pi}_k)$, and $\hat{\rho}_k = \mathrm{Tr}_b(\hat{\Pi}_k\hat{\rho}_{ab}\hat{\Pi}_k)/p_k$. This can be understood as the amount of information we can retrieve about one party (here, system a) by measuring the other one (system b). In general, the optimization is a difficult problem to address; however, for states of the form of Eq. (7), classical and quantum correlations can be solved analytically [33,34]. Specifically, it has been shown in Ref. [34] that the optimal observables for a real X state such as Eq. (7) correspond to σ_z if

$$(|r_{23}| + |r_{14}|)^2 \leqslant (r_{11} - r_{22})(r_{44} - r_{33}), \tag{13}$$

and correspond to σ_x if

$$|\sqrt{r_{11}r_{44}} - \sqrt{r_{22}r_{33}}| \leqslant |r_{23}| + |r_{14}|. \tag{14}$$

Under these conditions, expressions for discord in [33] are equivalent. In such case, the expression for the classical correlations is now given by

$$C(\hat{\rho}_{ab}) = S(\hat{\rho}_a) - \min_{\{\sigma_x,\sigma_y\}}[S(\hat{\rho}_{ab})|\{\sigma_x,\sigma_y\}], \tag{15}$$

where $S(\hat{\rho}_{ab})|\{\sigma_x,\sigma_y\}$ is the von Neumann entropy of $\hat{\rho}_{ab}$ when σ_x or σ_z has been measured in the subsystem b. When the minimum occurs for σ_x, we denote the classical correlations as $C(\hat{\rho_{ab}})|_{\sigma_x}$, while if the minimum is achieved by measuring σ_z, then we denote it as $C(\hat{\rho_{ab}})|_{\sigma_z}$ instead.

Let us consider the initial state (3), corresponding to an incoherent superposition of entangled coherent states. In Fig. 2, we show the evolution of correlations in the two-mode subsystem as a function of γt for (a) $\bar{n} = 1$ and for (b) $\bar{n} = 3$. As evidenced by the quantum mutual information (purple solid line) in Fig. 2(a), the overall system correlations decays smoothly as a consequence of decoherence. However, we can observe a sudden change in the dynamics of classical correlations and also in quantum discord at $t = t_s$. This tells us that there is a sudden change in the decoherence dynamics: Before t_s, decoherence has mostly a classical component (classical correlations decay faster than discord); after t_s, the roles are inverted and decoherence has mostly a quantum component. Despite this, decoherence still has mixed classical and quantum contributions, which is different from what has been found, for example, in Ref. [20], where the decoherence has either a quantum character or a classical one, but never both. On the other hand, Fig. 2(b) shows that by increasing the mean photon number $\bar{n}$ of the cavity modes, the classical correlations nearly freeze between γt_s and $\gamma t \approx 1$.

As we previously mentioned, when exploring the mesoscopic limit of a large number of photons in the cavity, interesting features in the dynamics are revealed. Such behavior is extended into quantum and classical correlations: This is clear in Fig. 3 where the dynamics of correlations is shown for $\bar{n} = 10$. In such figure, four dynamical regimes can be identified: Regime I is where classical correlations decay as a result of the decoherence process while discord is constant. Regime II is determined by a decaying discord and frozen classical correlations. In regime III, both discord and classical correlations attain a constant value, in particular discord vanishes. Finally, in regime IV, classical correlations start to decay again while discord shows a revival and then decays asymptotically to zero as all the energy in the cavities is transferred to the reservoirs.

The first regime (I) of the dynamics can be interpreted as follows: the decoherence only has a classical contribution since quantum correlations are frozen. Now, at the second regime (II), we found that the decoherence process now only has a quantum contribution. That is, regimes I and II are separated by a sudden transition from classical to quantum decoherence. So far, the dynamics of correlations resembles the results found in [20,25] for the case of qubits under the onset of dephasing.

Also, Fig. 3 shows that the time t_s, when the sudden transition from classical to quantum decoherence occurs, decreases with $\bar{n}$. This transition time, besides depending on $\bar{n}$, also depends on the parameter p of the initial mixed state given by Eq. (3). Using Eqs. (13) and (14), we find that this time t_s is given by

$$t_s = -\frac{1}{\gamma}\ln\left(1 + \frac{1}{4\bar{n}}\ln|2p-1|\right). \tag{16}$$

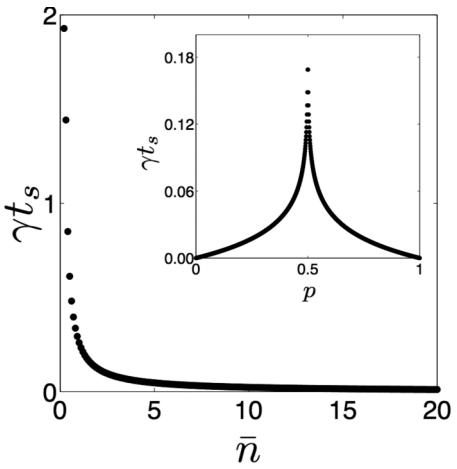

FIG. 4. Behavior of t_s as a function of the mean photon number $\bar{n}$ for $p = 0.3$ and as a function of p (inset) for $\bar{n} = 10$

Figure 4 shows the dependence of t_s on $\bar{n}$ and the initial-state parameter p. We can observe from the figure that the time t_s of the sudden transition from classical to quantum decoherence decays with $\bar{n}$ and also decays when the initial incoherent state (3) is more unbalanced, i.e., has more purity.

On the other hand, by analyzing the correlations dynamics in the strong-field case (Fig. 3), we find that in regime III of such case, both correlations are constant, i.e., neither discord nor classical correlations are affected by decoherence. Interestingly, this is true only in a finite-time span. This suggests that there is a time interval where the system settles in a time-dependent decoherence-free subspace. This time can be estimated from Eqs. (11), leading to $\Delta t = t_2 - t_1 = (1/\gamma)\ln(\bar{n} - 1)$. In this time interval, populations are constants. Moreover, coherences are also equals and constants; that is, in this stage, no decoherence is exhibited by the density matrix (7). After this finite-time interval, populations r_{22}, r_{33}, r_{44} and coherences r_{14} and r_{23} decay asymptotically to zero, while r_{11} goes to 1 since at $\gamma t \to \infty$ this density matrix element corresponds to the vacuum state population.

Furthermore, when classical correlations attained a constant value as in regimes II and III of the dynamics, it can be argued from its definition that measurements on the second qubit (cavity mode) project the system into a basis which is not affected by decoherence, that is, a *pointer-state basis* [22]. However, this pointer-state basis is not stable, as shown in regime IV in Fig. 3, where classical correlations return to decay, i.e., the system settles along regimes II and III in a metastable pointer state [24,25]. Notice that this occurs under a dissipative dynamics, which differs from the results shown in Ref. [22] where, in the amplitude damping case, no pointer states are found, but only in the dephasing case. Finally, in Fig. 3, we have plotted entanglement using concurrence [35] where we observe that entanglement suffers a sudden death [12,36] previous to t_s in regime I. Therefore, along the decoherence-free time span, no entanglement is present, which is consistent with previous results [24].

IV. SUMMARY

In summary, the dynamics of two initially correlated coherent states, each interacting with its own independent dissipative environment, has been analyzed. We found a sudden transition from classical to quantum decoherence since first the decoherence has only a classical component, given that discord is constant. Then only discord decays, meaning that decoherence is merely quantum. This sudden transition leads in the mesoscopic regime to the apparition of a metastable decoherence-free subspace. This is evidenced in the density matrix element, which does not evolve during a time span. The time when this sudden transition occurs is showed to be dependent on the average number of photons in each cavity and also on the purity of the initial state. The metastable decoherence-free subspace is linked to the metastability of a pointer basis where classical correlations between cavities are frozen. On the other hand, the size of the time interval depends mainly on the average number of photons in the cavities. This can also be understood in the context of pointer states: measurements on the second qubit (cavity mode) to calculate correlations projects the system into a basis which is not affected by decoherence.

ACKNOWLEDGMENTS

Authors acknowledge financial support from DICYT Grant No. 041631LC, Fondecyt Grant No. 1140194, and Financiamiento Basal FB 0807 para Centros Científicos y Tecnológicos de Excelencia.

[1] B. Groisman, S. Popescu, and A. Winter, Phys. Rev. A **72**, 032317 (2005).
[2] H. Ollivier and W. H. Zurek, Phys. Rev. Lett. **88**, 017901 (2001).
[3] L. Henderson and V. Vedral, J. Phys. A **34**, 6899 (2001).
[4] J. Oppenheim, M. Horodecki, P. Horodecki, and R. Horodecki, Phys. Rev. Lett. **89**, 180402 (2002).
[5] S. Luo, Phys. Rev. A **77**, 022301 (2008).
[6] S. Luo, Phys. Rev. A **77**, 042303 (2008).
[7] K. Modi, T. Paterek, W. Son, V. Vedral, and M. Williamson, Phys. Rev. Lett. **104**, 080501 (2010).
[8] B. P. Lanyon, M. Barbieri, M. P. Almeida, and A. G. White, Phys. Rev. Lett. **101**, 200501 (2008).
[9] K. Zyczkowski, P. Horodecki, M. Horodecki, and R. Horodecki, Phys. Rev. A **65**, 012101 (2001).
[10] L. Diósi, Lect. Notes Phys. **622**, 157 (2003).
[11] P. J. Dodd and J. J. Halliwell, Phys. Rev. A **69**, 052105 (2004).
[12] T. Yu and J. H. Eberly, Phys. Rev. Lett. **93**, 140404 (2004); **97**, 140403 (2006).
[13] M. F. Santos, P. Milman, L. Davidovich, and N. Zagury, Phys. Rev. A **73**, 040305(R) (2006).
[14] A. Shabani and D. A. Lidar, Phys. Rev. Lett. **102**, 100402 (2009).
[15] A. Datta and S. Gharibian, Phys. Rev. A **79**, 042325 (2009).
[16] M. Piani, M. Christandl, C. E. Mora, and P. Horodecki, Phys. Rev. Lett. **102**, 250503 (2009).

[17] T. Werlang, S. Souza, F. F. Fanchini, and C. J. Villas Boas, Phys. Rev. A **80**, 024103 (2009).
[18] J. Maziero, T. Werlang, F. F. Fanchini, L. C. Céleri, and R. M. Serra, Phys. Rev. A **81**, 022116 (2010).
[19] J. Maziero, L. C. Céleri, R. M. Serra, and V. Vedral, Phys. Rev. A. **80**, 044102 (2009).
[20] L. Mazzola, J. Piilo, and S. Maniscalco, Phys. Rev. Lett. **104**, 200401 (2010).
[21] J.-S. Xu, C.-F. Li, C.-J. Zhang, X.-Y. Xu, Y.-S. Zhang, and G.-C. Guo, Phys. Rev. A. **82**, 042328 (2010).
[22] M. F. Cornelio, O. J. Farías, F. F. Fanchini, I. Frerot, G. H. Aguilar, M. O. Hor-Meyll, M. C. de Oliveira, S. P. Walborn, A. O. Caldeira, and P. H. S. Ribeiro, Phys. Rev. Lett. **109**, 190402 (2012).
[23] T. Chanda, A. K. Pal, A. Biswas, A. Sen(De), and U. Sen, Phys. Rev. A **91**, 062119 (2015)
[24] C. E. López and F. Lastra, Phys. Rev A **96**, 062112 (2017).
[25] F. Lastra, C. E. López, S. A. Reyes, and S. Wallentowitz, Phys. Rev. A **90**, 062103 (2014).
[26] W. H. Zurek, Rev. Mod. Phys. **75**, 715 (2003).
[27] L. Davidovich, M. Brune, J. M. Raimond, and S. Haroche, Phys. Rev. A **53**, 1295 (1996).
[28] M. Brune, E. Hagley, J. Dreyer, X. Maitre, A. Maali, C. Wunderlich, J. M. Raimond, and S. Haroche, Phys. Rev. Lett. **77**, 4887 (1996).
[29] M. Penasa, S. Gerlich, T. Rybarczyk, V. Metillon, M. Brune, J. M. Raimond, S. Haroche, L. Davidovich, and I. Dotsenko, Phys. Rev. A **94**, 022313 (2016).
[30] S. P. Nolan and S. A. Haine, Phys. Rev. A **95**, 043642 (2017).
[31] S. Boixo, L. Viola, and G. Ortiz, Europhys. Lett. **79**, 40003 (2007).
[32] F. Lastra, G. Romero, C. E. López, N. Zagury, and J. C. Retamal, Opt. Commun. **283**, 3825 (2010).
[33] M. Ali, A. R. P. Rau, and G. Alber, Phys. Rev. A **81**, 042105 (2015).
[34] Q. Chen, C. Zhang, S. Yu, and X. X. Yi, and C. H. Oh, Phys. Rev. A **84**, 042313 (2011).
[35] W. K. Wootters, Phys. Rev. Lett. **80**, 2245 (1998).
[36] C. E. López, G. Romero, F. Lastra, E. Solano, and J. C. Retamal, Phys. Rev. Lett. **101**, 080503 (2008).